Synthesis, Structure, and Dynamics of Molybdenum Imido Alkyne Complexes

Elon A. Ison,[†] Thomas M. Cameron,[†] Khalil A. Abboud,[†] and James M. Boncella*[,†,‡]

Department of Chemistry and Center for Catalysis, University of Florida, P.O. Box 117200, Gainesville, Florida 32611-7200, and Nuclear Materials Technology Division, Los Alamos National Laboratory, Los Alamos, New Mexico 87545

Received January 21, 2004

The monomeric alkyne complexes (η^2-alkyne)Mo(NPh)(*o*-$(Me_3SiN)_2C_6H_4$) (**3**) have been synthesized by the displacement of isobutylene from (η^2-isobutylene)Mo(NPh)(*o*-$(Me_3SiN)_2$-C_6H_4) (**2**). The alkyne fragment in these complexes is oriented perpendicular to the Mo═N bond of the cis imido ligand, as confirmed by an X-ray structural analysis of **3e**. The deshielded nature of the chemical shifts of the α-carbons and terminal protons of the alkyne fragments in these complexes strongly suggests the participation of the alkyne $\pi_\perp$ electrons in the Mo−alkyne interaction. The alkyne fragment in **3** rotates freely about the Mo−alkyne bond, resulting in the fluxional behavior of these complexes at room temperature. An activation barrier of 13.2 kcal/mol for the alkyne rotation was measured using VT NMR spectroscopy. Computational studies using a two-layer ONIOM model, and the B3LYP hybrid functional, provided insight into the Mo−alkyne bonding. The transition state for alkyne rotation has been calculated and is characterized by a parallel orientation of the alkyne fragment to the cis imido ligand. A natural bond orbital (NBO) population analysis reveals that alkyne $\pi_\perp$ donation to Mo is more extensive in the transition state than in the ground state. Weaker Mo−N(imido) bonds are also observed in the transition state, because π donation from the alkyne ligand competes with imido π donation.

Introduction

Species containing transition-metal to ligand multiple bonds are widespread and play an important role in organometallic chemistry.[1] These species usually contain ligands such as imido, nitrene, oxo, and alkylidene that bind to the metal via overlap of the ligand p π and metal d π orbitals. When there are several π donors on a given metal center, ligand to metal π bonding results in a competition for available unfilled metal d orbitals. The term "π loading" has been used by Wigley and others to describe this phenomenon, and it has been suggested that the competition for metal π orbitals can lead to increased reactivity of organometallic complexes.[2−10]

While the structural and electronic effects of π loading are well documented for both tetrahedral and octahedral bis(imido) and mixed oxo−imido complexes,[11−13] there is a paucity of similar studies on the ability of alkyne ligands to compete as π donors on a given metal center in a π-loaded environment. It has been demonstrated, however, that alkynes can stabilize high oxidation states of transition metals via donation of their $\pi_\perp$ electrons.[14−17]

Recently, we have investigated the chemistry of group 6 imido complexes of the form M(NPh)(*o*-$(Me_3SiN)_2C_6H_4$)-X_2 (M = Mo, W) incorporating the *o*-pda (*o*-phenylenediamide) ligand.[18,19] This work has demonstrated that the diamide ligands are involved in a multicenter π-donor interaction with the metal center via the

* To whom correspondence should be addressed at Los Alamos National Laboratory, P.O. Box 1663, Mail Stop J-582, Los Alamos, NM 87545. E-mail: boncella@lanl.gov. Tel: (505) 665-0795. Fax: (505) 667-9905.

[†] University of Florida.

[‡] Los Alamos National Laboratory.

(1) Nugent, W. A.; Mayer, J. M. *Metal−Ligand Multiple Bonds*; Wiley: New York, 1988.

(2) Morrison, D. L.; Wigley, D. E. *Inorg. Chem.* **1995**, *34*(10), 2610−2616.

(3) Morrison, D. L.; Wigley, D. E. *J. Chem. Soc., Chem. Commun.* **1995**, (1), 79−80.

(4) Smith, D. P.; Allen, K. D.; Carducci, M. D.; Wigley, D. E. *Inorg. Chem.* **1992**, *31*(8), 1319−1320.

(5) Chao, Y. W.; Rodgers, P. M.; Wigley, D. E.; Alexander, S. J.; Rheingold, A. L. *J. Am. Chem. Soc.* **1991**, *113*(16), 6326−6328.

(6) Chao, Y. W.; Wexler, P. A.; Wigley, D. E. *Inorg. Chem.* **1989**, *28*(20), 3860−3868.

(7) Morrison, D. L.; Rodgers, P. M.; Chao, Y. W.; Bruck, M. A.; Grittini, C.; Tajima, T. L.; Alexander, S. J.; Rheingold, A. L.; Wigley, D. E. *Organometallics* **1995**, *14*(5), 2435−2446.

(8) Cundari, T. R. *Chem. Rev.* **2000**, *100*(2), 807−818.

(9) Benson, M. T.; Bryan, J. C.; Burrell, A. K.; Cundari, T. R. *Inorg. Chem.* **1995**, *34*(9), 2348−2355.

(10) Cundari, T. R. *J. Am. Chem. Soc.* **1992**, *114*(20), 7879−7888.

(11) Del Rio, D.; Montilla, F.; Pastor, A.; Galindo, A.; Monge, A.; Gutierrez-Puebla, E. *Dalton* **2000**(14), 2433−2437.

(12) Galindo, A.; Montilla, F.; Pastor, A.; Carmona, E.; Gutierrez-Puebla, E.; Monge, A.; Ruiz, C. *Inorg. Chem.* **1997**, *36*(11), 2379−2385.

(13) Montilla, F.; Pastor, A.; Galindo, A. *J. Organomet. Chem.* **1999**, *590*(2), 202−207.

(14) Templeton, J. L. *Adv. Organomet. Chem.* **1989**, *29*, 1−100.

(15) Birdwhistell, K. R.; Tonker, T. L.; Templeton, J. L. *J. Am. Chem. Soc.* **1987**, *109*(5), 1401−1407.

(16) Tatsumi, K.; Hoffmann, R.; Templeton, J. L. *Inorg. Chem.* **1982**, *21*(1), 466−468.

(17) Templeton, J. L.; Ward, B. C. *J. Am. Chem. Soc.* **1980**, *102*(9), 3288−3290.

(18) Ortiz, C. G.; Abboud, K. A.; Boncella, J. M. *Organometallics* **1999**, *18*(21), 4253−4260.

(19) Boncella, J. M.; Wang, S. Y. S.; Vanderlende, D. D.; Huff, R. L.; Abboud, K. A.; Vaughn, W. M. *J. Organomet. Chem.* **1997**, *530*(1−2), 59−70.

10.1021/om049942t CCC: $27.50
Publication on Web 07/21/2004

Scheme 1

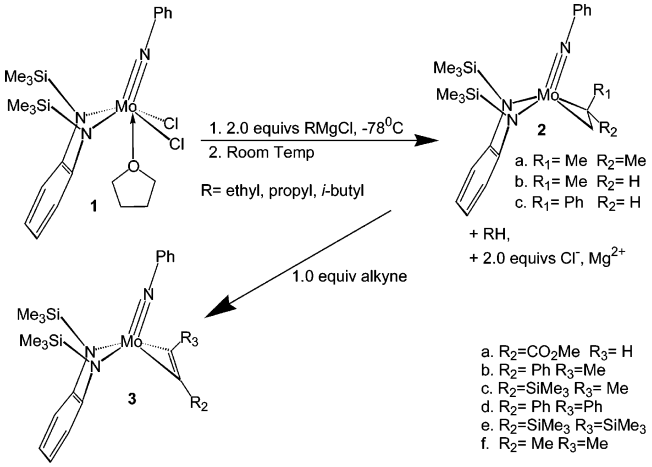

diamide lone-pair electrons. We originally observed the formation of a 2-butyne complex, (η^2-2-butyne)Mo(NPh)-(*o*-$(Me_3SiN)_2C_6H_4$), in the interaction of butadiene complexes with acetylenes.[20] The crystal structure of this complex was originally reported in this publication. The successful synthesis and isolation of high-oxidation-state complexes incorporating π-donor ligands[18] inspired us to complete our studies on the structure and bonding of alkyne ligands in group 6 imido diamido complexes. In so doing, we sought to answer the following question: can donation of the alkyne $\pi_\perp$ electrons effectively compete with the imido and diamide ligands on the metal center for empty metal d orbitals?

In this paper, we report the synthesis of the alkyne complexes (η^2-alkyne)Mo(NPh)(*o*-$(Me_3SiN)_2C_6H_4$) (**3**), along with the X-ray crystal structure of **3e**, and their solution behavior via low-temperature ^{1}H NMR spectroscopy. DFT calculations (B3LYP) have been used to study the bonding in these complexes, and an NBO analysis was used to determine the extent of π donation by the alkyne ligand.

Results and Discussion

Synthesis of Alkyne Complexes. Base-free molybdenum alkyne complexes of the type [η^2-(alkyne)Mo-(NPh)-*o*-$(Me_3SiN)_2C_6H_4$)] (**3**) were prepared by treating pentane solutions of **2** with the appropriate alkyne, followed by removal of solvent under reduced pressure (Scheme 1). The alkyne reactants displace the bound olefin with complete conversion to products within 15 min at 20 °C. The ^{1}H NMR spectra of **3** are consistent with monomeric alkyne complexes. As shown in Table 1, the ^{13}C NMR resonances of the α-carbons of the alkyne fragment are significantly deshielded, suggesting the involvement of the alkyne $\pi_\perp$ electrons in the M−alkyne bonding.[14−16,21−24] Alkyne complexes **3a**−**e** are air sensitive but stable in solution and in the solid state. In contrast, the alkyne complex **3f** is unstable and decomposes in solution at −40 °C within ca. 12 h.

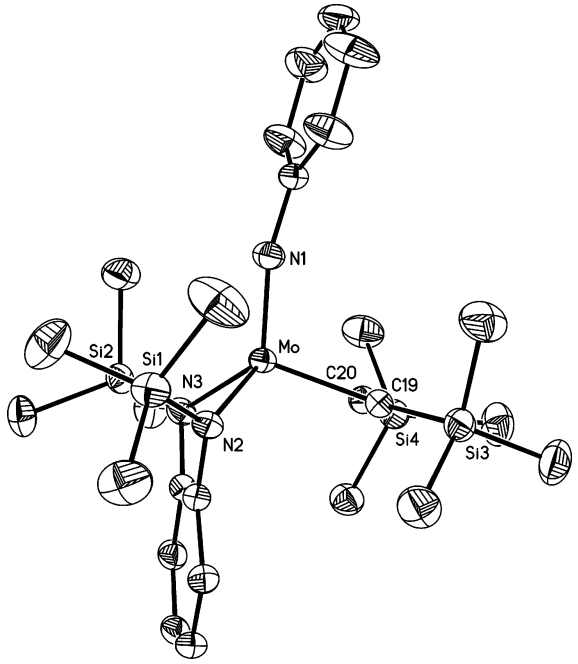

Figure 1. Thermal ellipsoid plot of **3e**, [Mo(NPh)(η^2-bis-(trimethysilyl)acetylene){*o*-$(Me_3SiN)_2C_6H_4$}] (40% probability thermal ellipsoids). Selected bond lengths (Å): Mo−N(1), 1.745(2); Mo−N(2), 2.023(2); Mo−N(3), 2.009(2); Mo−C(19), 2.078(3); Mo−C(20), 2.079(3); C(19)−C(20), 1.305(4).

Table 1. ^{1}H and ^{13}C NMR Data for Alkyne Complexes

			^{13}C NMR, ppm		^{1}H NMR,	T_c,	$\Delta G^\ddagger$,
complex	R_2	R_3	C_1	C_2	ppm	K	kcal/mol
3a	CO_2Me	H	175	177	9.2	257	13.2
3b	Ph	Me	185	180		268	13.4
3c	$SiMe_3$	Me	200	181		268	13.4
3d	Ph	Ph	180				
3e	$SiMe_3$	$SiMe_3$	205				
3f	Me	Me	187				

A single-crystal X-ray analysis was performed on a single crystal of **3e**. As shown in the thermal ellipsoid plot in Figure 1, the alkyne complex adopts a pseudo-square-pyramidal structure with the imido ligand occupying the apical position. The alkyne ligand is oriented perpendicular to the cis imido ligand, and the Mo−C(19) and Mo−C(20) bond lengths, 2.078 and 2.079 Å, respectively, are consistent with Mo−C single bonds. The C(19)−C(20) bond length for **3e**, 1.305 Å, is close to the generally accepted value for C−C double bonds. Pronounced back-bonding is responsible for the lengthening of this alkyne bond, and the structure of **3e** is thus best described as having a large contribution from a metallacyclopropene structure. In this resonance form, the alkyne ligand can be considered as a dianionic ligand and the formal oxidation state of the metal would be best described as Mo(VI).

In addition, the diamide ligand is folded through concerted torsion of the NR group about the C−N bond of the pda ring. The fold angle (angle between the N(2)-MoN(3) plane and the plane of the pda ring) is 133°. This folding has been attributed to donation of the

(20) Cameron, T. M.; Ghiviriga, I.; Abboud, E. A.; Boncella, J. M. *Organometallics* **2001**, *20*(21), 4378−4383.
(21) Crane, T. W.; White, P. S.; Templeton, J. L. *Inorg. Chem.* **2000**, *39*(6), 1081−1091.
(22) Crane, T. W.; White, P. S.; Templeton, J. L. *Organometallics* **1999**, *18*(10), 1897−1903.
(23) Templeton, J. L.; Herrick, R. S.; Morrow, J. R. *Organometallics* **1984**, *3*(4), 535−541.
(24) Herrick, R. S.; Templeton, J. L. *Organometallics* **1982**, *1*(6), 842−851.

Table 2. Fold Angles for Mo Imido Diamido Complexes

molecule	fold angle (deg)
(η^2-bis(trimethylsilyl)acetylene)Mo-(NPh)(*o*-$(Me_3SiN)_2C_6H_4$)[20]	133.0
(η^2-2-butyne)Mo(NPh)(*o*-$(Me_3SiN)_2C_6H_4$)	133.0
Mo(NPh)(*o*-$(Me_3SiN)_2C_6H_4$)$(CH_2)_4$[30]	132.5
(η^2-styrene)Mo(NPh)(*o*-$(Me_3SiN)_2C_6H_4$)[30]	129.2
cis-$(pyridine)_2$Mo(NPh)(*o*-$(Me_3SiN)_2C_6H_4$)[31]	175.5
(η^4-butadiene)Mo(NPh)(*o*-$(Me_3SiN)_2C_6H_4$)[20]	167.8

diamide lone-pair electrons into the empty metal d_{xy} orbital.[25−29]

Computational and structural studies on d^0 diamide imido complexes have demonstrated the importance of diamide lone-pair donation in the bonding in these complexes. In these structures, the diamide lone-pair electrons are donated to an empty metal d orbital of appropriate symmetry through concerted torsion of the sp^2 nitrogens in order to achieve effective lone-pair p−d overlap. This torsion results in the folding of the *o*-pda ligand, as depicted in Table 2.

It is evident from Table 2 that there is a distinct correlation between the fold angle of the diamide ligand and the oxidation state of the metal. In d^0 dialkyl complexes such as the metallacyclopentane complex Mo(NPh)(*o*-$(Me_3SiN)_2C_6H_4$)$(CH_2)_4$, the diamide ligand is considerably folded. Table 2 also shows that in the alkyne complexes **3e**,**f** and the styrene complex [η^2-(styrene)Mo(NPh)-*o*-$(Me_3SiN)_2C_6H_4$)][30] the diamide ligand folds to an extent that is comparable to that in the metallacyclopentane complex, where the oxidation state of the metal is unambiguously assigned as Mo(VI).

In contrast, the folding of the diamide ligand is minimized in d^2 complexes such as the pyridine complex [*cis*-$(pyridine)_2$Mo(NPh)(*o*-$(Me_3SiN)_2C_6H_4$)],[31] and the butadiene complex [(η^4-butadiene)Mo(NPh)(*o*-$(Me_3SiN)_2$-C_6H_4)],[20] where the oxidation state of the metal is assigned as Mo(IV). The synthesis and characterization of these complexes have been reported elsewhere. It is clear from Table 2 that the electronic properties of the metal dictate the extent of diamide folding.

Significant π back-bonding in the alkyne and olefin complexes results in a significant charge transfer from Mo to the alkyne or olefin, and these complexes are best described as d^0 metallacyclopropene and metallacyclopropane complexes, respectively. The C−C bond lengths of the alkyne in these complexes are significantly longer than in typical Mo(IV) complexes that incorporate the alkyne imido moiety oriented perpendicular to the imido fragment. For example, the C−C bond lengths of the Mo(IV) complexes Mo(Ntol)(DMAC)$(S_2CNEt_2)_2$[32] (where DMAC = dimethyl acetylenedicarboxylate) and [$MoCl_2$-{N(mes)}(PhCCPh)$(PMe_3)_2$][33] are significantly shorter (1.264 and 1.251 Å, respectively) than those found in **3e**,**f** and reflect the fact that π donation from Mo in **3e**,**f** is significant and results in a substantial reduction of the bond order of the alkyne ligand.

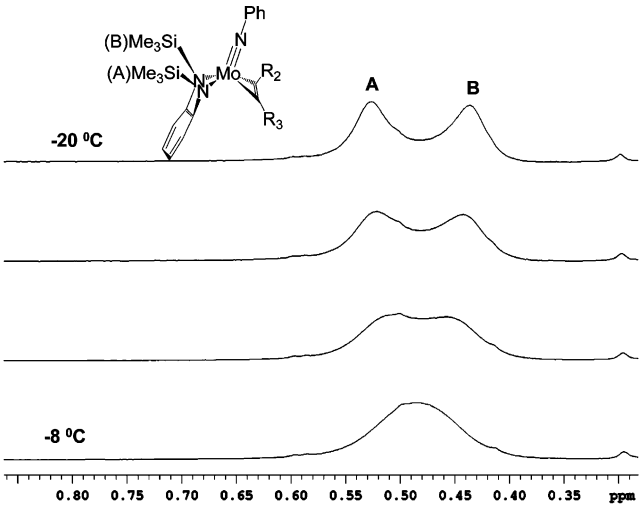

Figure 2. Variable-temperature ^1H NMR spectrum from −20 to −8 °C for complex **3b**.

In solution, the alkyne complexes exhibit C_s symmetry, just as in the solid state. In complexes **3d**−**f**, where the alkyne substituents are the same, a plane of symmetry bisecting the C−C bond of the alkyne, containing the NMo bond of the imido ligand, and bisecting the *o*-pda ring causes the $SiMe_3$ protons to become chemically equivalent and they appear as a broad peak at 0.4−0.6 ppm. However, in complexes **3a**−**c**, where the alkyne substituents are different, there is no longer a plane of symmetry and the $SiMe_3$ protons are no longer equivalent. These protons appear as a broad singlet in the ^1H NMR spectra at room temperature. However, cooling a C_7D_8 solution to −50 °C results in the splitting of this peak into two singlets (Figure 2). The activation barrier for this process has been measured to be 13.2 kcal/mol. Interestingly, the barrier is the same regardless of the alkyne substituent (Table 1).

This fluxional process can be explained by rotation of the alkyne fragment about the Mo−alkyne centroid axis. This motion takes the alkyne ligand through a transition state that is also of C_s symmetry (Scheme 2) where the alkyne is oriented parallel to the imido ligand.

Molecular Orbital Calculations. To elucidate the bonding pattern of the alkyne fragment in these complexes, density functional theory calculations (DFT) were performed. Initial calculations were carried out on model compound **4** (Figure 3), which is a simplified version of **3** where the *o*-phenylene group (*o*-C_6H_4) that links the two N atoms of the diamido ligand was reduced to a −CH=CH− carbon chain. The organic groups on the nitrogen atoms ($SiMe_3$ of the amido and phenyl group of the imido) were replaced by hydrogen atoms for simplicity. Propyne was used as the alkyne fragment in this model. The calculated structure for **4** is generally in good agreement with the X-ray crystal structure data

(25) Wang, S. Y. S.; Abboud, K. A.; Boncella, J. M. *J. Am. Chem. Soc.* **1997**, *119*(49), 11990−11991.
(26) Del Rio, D.; Galindo, A. *J. Organomet. Chem.* **2002**, *655*(1−2), 16−22.
(27) Galindo, A.; Gomez, M.; Del Rio, D.; Sanchez, F. *Eur. J. Inorg. Chem* **2002**(6), 1326−1335.
(28) Galindo, A.; Ienco, A.; Mealli, C. *New J. Chem.* **2000**, *24*(2), 73−75.
(29) Galindo, A.; Ienco, A.; Mealli, C. *Comments Inorg. Chem.* **2002**, *23*(6), 401−416.
(30) Cameron, T. M.; Ortiz, C. G.; Ghiviriga, I.; Abboud, K. A.; Boncella, J. M. *Organometallics* **2001**, *20*(10), 2032−2039.
(31) Cameron, T. M.; Abboud, K. A.; Boncella, J. M. *Chem. Commun.* **2001**(13), 1224−1225.
(32) Devore, D. D.; Maatta, E. A. *Inorg. Chim. Acta* **1985**, *112*(1), 87−91.
(33) Montilla, F.; Galindo, A.; Carmona, E.; Gutierrez-Puebla, E.; Monge, A. *J. Chem. Soc., Dalton Trans.* **1998**, 1299−1305.

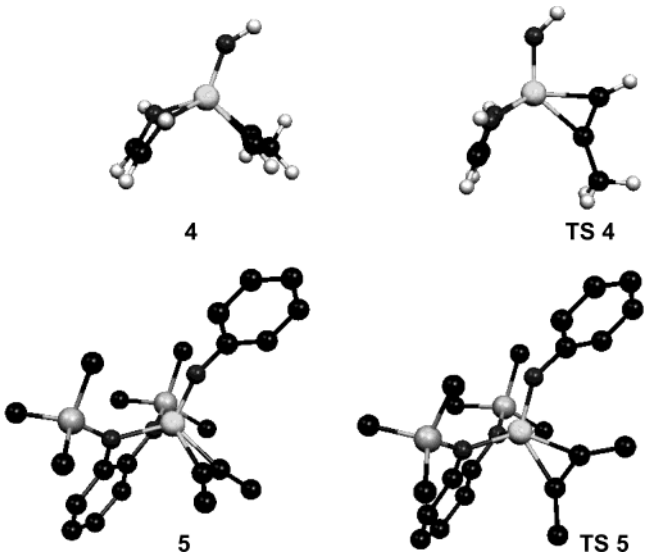

Figure 3. B3LYP optimized models for alkyne complexes and the transition states for alkyne rotation.

Scheme 2

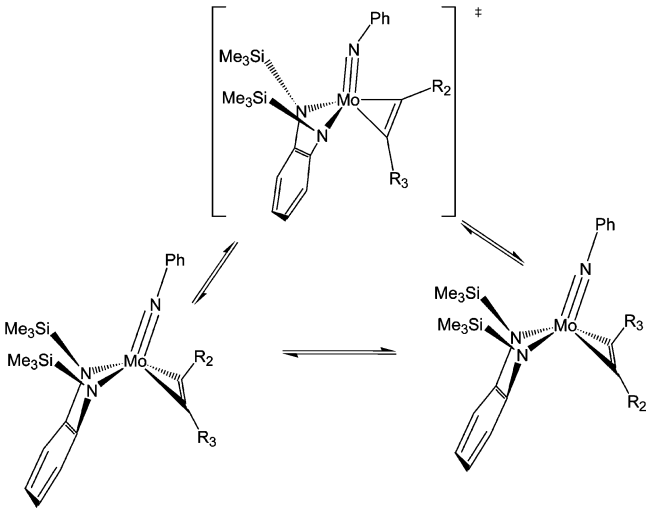

obtained for **3e**,**f**.[20] The only exception is that the ligand is significantly less folded in this model than in the actual compounds (147° vs 133°). This is due to the inability of the hydrogen atoms on the diamide ligand to successfully model the bulky $SiMe_3$ groups.

To obtain a more accurate model for the alkyne complexes, we employed the ONIOM approach developed by Morokuma et al.[34] to model the complete ligand system with all substituents used in the experiment (Figure 3). We defined a two-layer model: model compound **5**, for the 2-butyne complex **3f**. The outer layer consisted of the entire complex, including the entire *o*-pda ligand, and phenyl and $SiMe_3$ substituents on the imido and diamide ligand, respectively, and the inner layer was comprised of **4**, with acetylene as the alkyne fragment. The inner layer was modeled using the B3LYP/lanl2dz basis set, while the B3LYP/lanl2mb basis set was used to model the substituents. As shown in Table 3, there is good agreement between the calculated structure **5** and the X-ray crystal structure for **3f**.

(34) Dapprich, S.; Komaromi, I.; Byun, K. S.; Morokuma, K.; Frisch, M. J. *J. Mol. Struct. (THEOCHEM)* **1999**, *462*, 1−21.

Table 3. Comparison of Selected Bond Lengths (Å) and Angles (deg) between Model Compounds 4 and 5 and the Reported Crystal Structure for 3f[a]

	theor				exptl	
param	**4**	**TS 4**	**5**	**TS 5**	**3e**	**3f[a]**
Mo−N(1)	1.755	1.798	1.776	1.818	1.745(2)	1.751(2)
Mo−N(2)	2.018	2.053	2.003	2.005	2.009(2)	2.031(2)
Mo−N(3)	2.018	2.037	2.020	1.991	2.022(2)	2.001(2)
Mo−C(19)	2.087	2.089	2.086	2.087	2.078(3)	2.056(2)
Mo−C(20)	2.071	2.079	2.083	2.075	2.079(3)	2.052(2)
C(19)−C(20)	1.331	1.346	1.333	1.353	1.305(4)	1.297(3)
fold angle[b]	147	141	137	138	133	133

[a] See ref 21 for crystallographic information. [b] The fold angle is defined as the angle between the planes made by Mo, N(2), and N(3) and the plane defined by the benzenoid portion of the *o*-pda ring.

Scheme 3

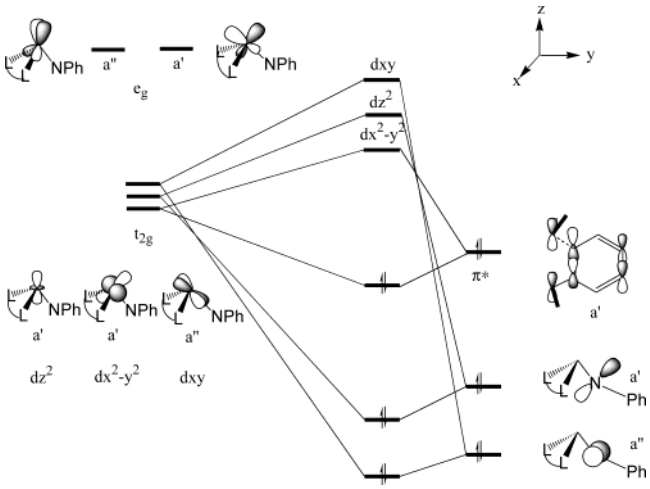

The transition states corresponding to alkyne rotation about the Mo−alkyne bond in both **4** and **5** have been located. In both of these transition states the alkyne ligand is now oriented parallel to the Mo−imido bond. This involves rotation of the alkyne ligand in **4** and **5** by 90° about the Mo−alkyne bond. The activation energy $\Delta E^{\ddagger}$ (where $\Delta E^{\ddagger}$ refers to electronic energy differences and does not include the zero point correction) obtained from these calculations is 16.9 kcal/mol for the rotation of **4** and 14.4 kcal/mol for the rotation of **5**. These values compare favorably to the experimentally obtained activation barrier of 13.2 kcal/mol.

To better understand the nature of the bonding in these complexes, we undertook a qualitative MO analysis and applied Weinhold's natural bond orbital (NBO) method to the complex. Scheme 3 shows the effects of the consideration of π contributions of the diamide and imido ligands (right side) on a typical ML_3 fragment (left side). In this nonstandard orientation the metal d orbitals have a composition different from that usually used for octahedral complexes. This is due to the coordinate system shown in the top right corner of this scheme. In a pure ML_3 fragment the *z* axis coincides with a 3-fold rotational axis of an octahedron. The atomic compositions of the metal d orbitals are mixed so that the orbitals are reorientated to lay between the M−L bonds. For example, the a′ component of the e_g

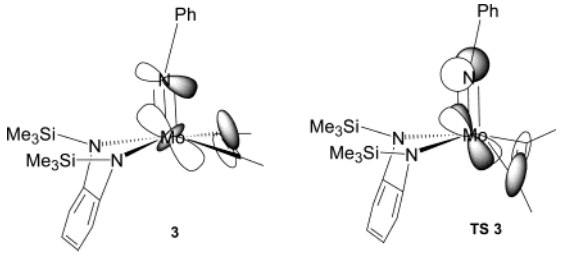

Figure 4. Bonding interactions between Mo, imido, and the alkyne fragment.

set becomes $\sqrt{1/3}(x^2 - y^2) + \sqrt{2/3}(yz)$. For full details on the atomic composition of a pure ML_3 fragment see ref 35.

The metal t_{2g} orbitals in this nonstandard orientation are comprised of one orbital of a″ symmetry, primarily d_{xy}, and two orbitals of a′ symmetry, primarily $d_{x^2-y^2}$, and d_{z^2}. The metal e_g orbitals become a″, primarily d_{yz}, and a′, primarily d_{xz}. In the case of Mo the three t_{2g}-derived orbitals lie relatively high in energy and above the diamide chelate's populated π^* orbital. The two filled orthogonal p_π orbitals on the imido nitrogen destabilize the metal t_{2g} orbitals of a′ (d_{z^2}) and a″ (d_{xy}) symmetry. The $d_{x^2-y^2}$ orbital remains closest in energy to the diamide chelate's populated π^* orbital, and it is this interaction that is responsible for the folding of the diamide ligand.

Donor electrons on the alkyne alter the MO diagram in Scheme 3. These electrons compete for empty metal orbitals with the imido ligand: for example, the alkyne $\pi_\perp$ electrons compete with the imido ligand for the metal d_{z^2} orbital in the ground state and the d_{xy} orbital in the transition state, resulting in a three-center−four-electron bonding interaction between the imido group, the metal center, and the alkyne ligand. These bonding combinations are depicted pictorially in Figure 4.

NBO Population Analysis. More detailed information about the alkyne→metal π interactions can be obtained from an NBO population analysis. The NBO[36−38] program diagonalizes the one- and two-center blocks of the first-order reduced density matrix in such a way that natural bonds are obtained that are said to represent the best Lewis structure of a molecule. This involves a sequence of transformations from a given basis set to various localized sets: natural atomic orbitals (NAOs), natural hybrid orbitals (NHOs), natural bond orbitals (NBOs), and natural localized molecular orbitals (NLMOs). The NLMOs can then be transformed to occupied MOs. Delocalization effects appear as weakly occupied antibonding or Rydberg orbitals.

Lewis structures obtained from NBO analyses accounted for approximately 97% of the electron density. As shown in Table 4, the NLMO analysis can be used to quantify the delocalization of the alkyne $\pi_\perp$ electrons. In the transition states **TS 4** and **TS 5,** a greater proportion of the electron density of the parent NBO of the alkyne C−C π bond is delocalized onto molybdenum.

Table 4. NLMO Analysis of the Alkyne π Bond

model	% π C−C	% Mo	occ
4	86.9	9.2	1.738
TS 4	80.1	13.8	1.660
5	86.9	8.5	1.738
TS 5	78.9	14.0	1.640

Table 5. NBO Analysis of the Mo−N(imido) Bonds

model	bond type	% Mo	% N	occ	covalent bond order[b]
4	σ	22.9	77.1	1.94	0.960
	π_1	27.3	72.7	1.83	
	π_2	31.7	68.3	1.90	
5	σ	26.2	73.8	1.97	0.949
	π_1	22.1	77.9	1.76	
	π_2	31.6	68.4	1.83	
TS 4	σ	37.9	62.1	1.97	0.928
	π_1	39.3	60.7	1.92	
	n[a]	6.4	89.5	1.80	
TS 5	σ	37.1	62.9	1.92	0.868
	π_1	36.4	63.6	1.88	
	n[a]	6.7	86.5	1.74	

[a] n = lone pair. [b] Atom−atom overlap-weighted NAO bond order.

In addition, the occupancy of this bond is also lower in the transition state.

Table 5 shows the population analysis of the Mo−imido bond. The bond type, percent contribution from each atom, and occupancy of each chemical bond are presented. The Mo−N(imido) bond in model complexes **4** and **5**, where the alkyne is aligned in an orthogonal orientation, consists of a σ-bond and two π-bonds, as would be expected for a metal−nitrogen triple bond. All bonds are substantially polarized toward nitrogen with 68−77% contributions from nitrogen and 22−32% from molybdenum.

However, this bond in transition state structures **TS 4** and **TS 5** consists of one σ-bond and one π-bond; the third π-bond is significantly localized on the nitrogen atom (N contribution 87−90%) and is best described as a lone pair with some delocalization onto the molybdenum center (6.4−6.8%). These data, in addition to the lower covalent bond orders of the Mo−N bonds for model complexes **4** and **5** (Table 4), suggests a weakening of the Mo−N(imido) bonds in the transition state. The weakening of the Mo−N (imido) bond is also reflected in the lengthening of this bond in the transition state from 1.755 to 1.798 Å for the rotation of **4** to **TS 4** (Table 4). Increased donation of the $\pi_\perp$ electrons in the TS is also reflected by a weakening of the C−C bond in the transition state (Table 4).

The NLMOs of **4** and **TS 4** are represented pictorially in Figure 5. The larger contributions of the Mo d−π orbital in the transition state **TS 4** is evident in Figure 5h versus the significantly smaller contributions from these orbitals in Figure 5d. Also, the localization of the third Mo−N(imido) π bond is evident in Figure 5g. Thus, it is only in the transition state that the alkyne π electrons compete effectively for metal d orbitals. This is evidently a higher energy process, as the stronger metal−nitrogen π bonds are replaced by weaker metal−carbon π bonds, leading to the observed activation barrier associated with alkyne rotation.

Summary and Conclusions. We have demonstrated the synthesis of novel high-oxidation-state molybdenum imido alkyne complexes that show significant interactions between the alkyne $\pi_\perp$ electrons and the metal

(35) Albright, T. A.; Burdett, J. K.; Whangbo, M. *Orbital Interactions in Chemistry*; Wiley: New York, 1985; p 383.
(36) Glendening, E. D.; Reed, A. E.; Carpenter, J. E.; Weinhold, F. NBO Version 3.1.
(37) Weinhold, F. *J. Chem. Educ.* **1999**, *76*(8), 1141−1146.
(38) Reed, A. E.; Curtiss, L. A.; Weinhold, F. *Chem. Rev.* **1988**, *88*(6), 899−926.

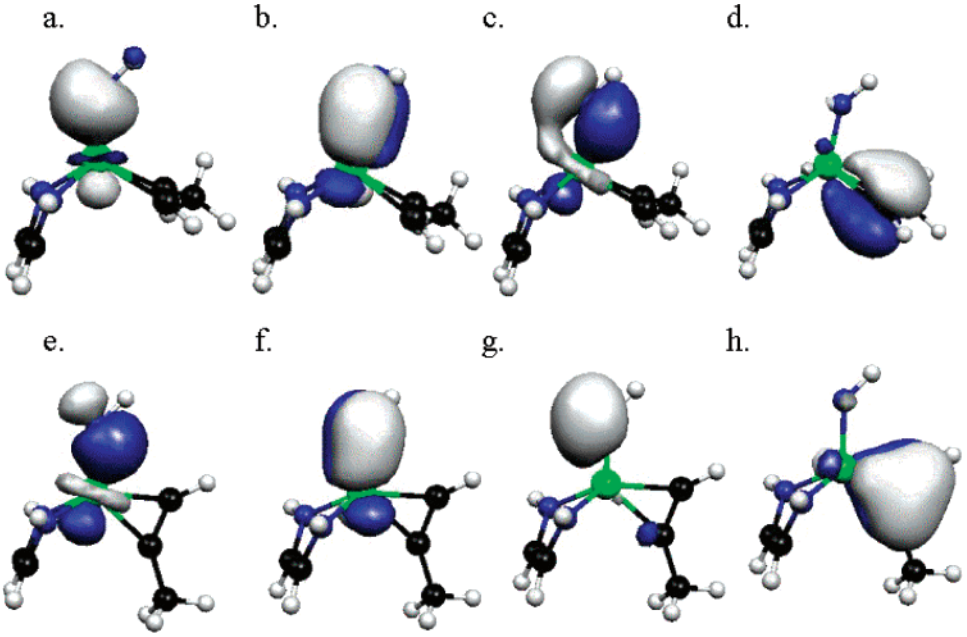

Figure 5. (a−c) NLMO plots (isocontour 0.04) of the Mo−N(imido) bond in **4**: (a) imido−Mo d_{z^2} (σ); (b) imido−Mo (d_{z^2}, d_{yz} hybrid, π); (c) imido−Mo (d_{xy}, π). (e-g) NLMO plots (isocontour 0.04) of the Mo−N(imido) bond in **TS 4** (e−g): (e) imido−Mo d_{z^2} (σ); (f) imido−Mo (d_{xy}, π); (g) imido lone pair. Plot d is the C−C π bond−Mo(d_{z^2}, d_{yz} hybrid) in **4**, and plot h is the C−C π bond−Mo (d_{xz}, d_{xy} hybrid) in **TS 4**.

center. The implications of this interaction on the structure and dynamics of these complexes have been explored via DFT (B3LYP) and NBO calculations. These calculations reveal that the alkyne π donation in these complexes occurs at the expense of Mo−N(imido) bonding. This is an unfavorable interaction, since the stronger Mo−N bonds are replaced by weaker Mo−C bonds. The perpendicular orientation of the alkyne ligand in the ground state of these complexes arises as the molecule minimizes the alkyne to Mo π donation and maximizes the imido to Mo π donation. It is clear that the interplay of π donor ligands in this class of compounds plays a crucial role in determining their properties and suggests that a judicious choice of the π donors may offer a way to modify the chemistry of these compounds in a desirable fashion.

Experimental Section

All operations were conducted under an inert atmosphere using standard Schlenk techniques or in a nitrogen-filled drybox. Diethyl ether, pentane, toluene, and tetrahydrofuran were distilled under nitrogen from sodium or sodium benzophenone ketyl, stored over molecular sieves, and degassed prior to use. Ethylene was predried by passing the gas through a column of molecular sieves. NMR spectra were recorded on Varian (300 MHz) Gemini300, VXR300, and Mercury300 instruments. Chemical shifts are reported in ppm relative to the ^{1}H and ^{13}C residues of the deuterated solvents. Elemental analyses were performed by Complete Analysis Laboratories Inc., Parsipanny, NJ.

Synthesis of η^2-Alkyne Complexes. R_1 = H, R_2 = CO_2Me (3a). Methyl propiolate (0.17 mL, 1.94 mmol) was added dropwise with stirring to a pentane solution of **2a** (0.959 g, 1.94 mmol). An immediate color change from green to orange occurred. The reaction mixture was stirred for $^1/_2$ h, after which the solution was concentrated by removal of the solvent in vacuo. The pentane solution was reduced to ca. 10 mL and then cooled to −78 °C for 2 h. Orange crystals appeared, and after filtration [Mo(NPh)(η^2-methyl propiolate){*o*-(Me_3SiN)$_2$-C_6H_4}] (**3a**) was obtained in 82% yield. Recrystallization from concentrated pentane solutions of **3a** allowed for further purification. Complex **3a** is not stable in solution at 20 °C and decomposes in solution at −30 °C overnight. It can be stored as a solid under an inert atmosphere at −40 °C.[13] Due to the thermal instability of **3a** elemental analysis was not possible. ^{1}H NMR (C_7D_8, 20 °C): δ 9.13 (s, 1H, alkyne proton), 7.33 (d, 2H, J = 8.1 Hz, phenyl imido ortho protons), 7.20 (bs, 2H, *o*-pda ring protons), 6.80 (t, 1H, phenyl imido para proton, J = 7.7 Hz), 3.44 (s, 3H, CO_2Me protons), 0.48 (s, 18H, $SiMe_3$ protons). One *o*-pda resonance and one phenyl imido resonance are overlapping with solvent. ^{1}H NMR (C_7D_8, −50 °C): δ 9.08 (s, 1H, alkyne proton), 7.42 (d, 2H, J = 7.2 Hz, phenyl imido ortho protons), 7.27 (d, 2H, J = 7.8 Hz, *o*-pda ring protons), 6.93 (t, 1H, J = 7.5 Hz, phenyl imido meta proton), 6.80 (t, 1H, J = 7.5 Hz, phenyl imido para proton), 3.42 (s, 3H, CO_2-Me protons), 0.49 (s, 9H, $SiMe_3$ protons), 0.45 (s, 9H, $SiMe_3$ protons). One *o*-pda resonance is overlapping with solvent. ^{13}C NMR (C_6D_6, 20 °C): δ 1.8, 51.8, 122.9, 124.1, 125.7, 126.2, 129.3, 133.4, 138.3, 157.6, 173.8, 176.8.

R_1 = Ph, R_2 = Me (3b). 1-Phenyl-1-propyne was added dropwise with stirring to a pentane solution of **2a** (1.00 g, 2.026 mmol). An immediate color change from green to orange occurred. The reaction mixture was stirred for $^1/_2$ h, after which the solution was concentrated by removal of the solvent in vacuo. The pentane solution was reduced to ca. 10 mL and then cooled to −78 °C for 2 h. Orange crystals appeared, and after filtration [Mo(NPh)(η^2-1-phenyl-1-propyne){*o*-(Me_3SiN)$_2$$C_6H_4$}] (**3b**) was obtained in 84% yield. Recrystallization from concentrated pentane solutions of **3b** allowed for further purification. ^{1}H NMR (C_6D_6, 20 °C): δ 7.36 (d, 2H, phenyl imido ortho protons) 7.35 (d, 2 H, alkyne phenyl ortho proton, J = 8.1 Hz, 4.9 Hz), 7.24 (bs, 2H, *o*-pda ring protons), 7.14 (t, 2H, phenyl imido meta proton, J = 6.6 Hz), 7.04 (t, 2H, alkyne phenyl meta proton, J = 7.5 Hz), 7.00 (t, 1H, phenyl imido para proton, J = 6.3 Hz), 6.91 (s, o-pda ring protons), 6.80 (t, 1H, J = 7.4 Hz, alkyne phenyl para proton), 2.41 (s, 3H, CH_3-CCPh protons), 0.48 (s, 18H, $SiMe_3$ protons). ^{1}H NMR (C_7D_8, −40 °C): δ 7.38 (d, 2H, J = 9.0 Hz, phenyl imido ortho proton), 7.35 (d, 2H, J = 8.0 Hz, alkyne phenyl ortho protons), 7.11 (t, 2H, J = 8.2 Hz, alkyne phenyl meta protons), 6.88 (dd, 2H, J

= 6.4 Hz, 2.4 Hz, *o*-pda ring protons), 6.83 (t, 1H, J = 8.2 Hz, alkyne phenyl para proton), 6.77 (t, 1H, J = 7.2 Hz, phenyl imido para proton), 2.40 (s, 3H, PhCCMe proton), 0.52 (s, 9H, $SiMe_3$), 0.43 (s, 9H, $SiMe_3$). ^{13}C NMR (C_6D_6, 20° C): δ 2.4, 18.9, 122.9, 123.8, 124.5, 127.9, 128.8, 129.2, 129.8, 139.5, 158.2, 179.9, 185.4. Anal. Calcd for $C_{27}H_{35}MoN_3Si_2$: C, 58.57; H, 6.37; N, 7.59. Found: C, 58.44; H, 6.35; N, 7.52.

R_1 = $SiMe_3$, R_2 = Me (3c). One equivalent of (trimethylsilyl)propyne was added dropwise with stirring to a pentane solution of **2a** (0.47 g, 0.95 mmol). The reaction mixture was stirred for $^1/_2$ h, after which the solution was concentrated by removal of the solvent in vacuo. The pentane solution was reduced to dryness and [Mo(NPh)(η^2-(trimethylsilyl)propyne)-{*o*-$(Me_3SiN)_2C_6H_4$}] (**3c**) was obtained as a green oil in 95% yield. Further attempts to recrystallize this compound were unsuccessful. ^1H NMR (C_6D_6, 20 °C): δ 0.44 (s, 9H, $SiMe_3$), 0.46 (s, 18H, $SiMe_3$), 2.44 (s, 3H, Me), 6.82−7.33 (aromatics), 10.11 (s, 1H, alkyne). ^1H NMR (C_6D_6, −50 °C): 7.33 (d, 2H, J = 7.8 Hz, phenyl imido ortho protons), 7.22 (m, 2H, *o*-pda ring protons), 7.04 (t, 2H, J = 8.2 Hz, phenyl imido meta protons), 6.91 (dd, 2H, J = 7.8 Hz, 3.6 Hz, *o*-pda ring protons), 6.80 (t, 1H, J = 7.5 Hz, phenyl imido para proton), 2.45 (s, 3H, $SiMe_3$-CCMe protons), 0.51 (s, 9H, $SiMe_3$ protons), 0.48 (s, 9H, $SiMe_3$ protons), 0.23 (s, 9H, $SiMe_3$ protons). ^{13}C NMR δ 0.2, 2.03, 20.7, 123.4, 124.0, 128.7, 157.8, 180.7, 199.6.

R_1 = Ph, R_2 = Ph (3d). To a stirred solution of **2a** (0.590 g, 1.195 mmol) in pentane was added diphenylacetylene (0.213 g, 1.195 mmol). The reaction mixture was stirred overnight, and **3d** was isolated as a red solid upon concentration of the reaction mixture under reduced pressure (yield 77%). ^1H NMR (C_6D_6, 20 °C): δ 0.42 (Si*Me*$_3$, 18 H), 6.8−7.4 (ov, mult, 19 H). ^{13}C NMR (C_6D_6, 20 °C): δ 2.1, 122.9, 123.6, 124.6, 125.2, 128.5, 128.7, 129.0, 134.1, 139.8, 157.8, 182.0. Anal. Calcd for $C_{32}H_{37}MoN_3Si_2$: C, 62.42; H, 6.06; N, 6.82. Found: C, 62.11; H, 6.41; N, 6.46.

R_1= $SiMe_3$, R_2 = $SiMe_3$ (3e). To a stirred solution of **2a** (0.910 g, 1.840 mmol) in pentane was added bis(trimethylsilyl)-acetylene (0.307 g, 1.840 mmol). The reaction mixture was stirred overnight, and **3e** was isolated as a green solid upon concentration of the reaction mixture under reduced pressure (yield 77%). ^1H NMR (C_6D_6, 20 °C): δ 0.22 (Si*Me*$_3$, 18 H), 0.41 (Si*Me*$_3$, 18 H), 6.08 (t of t, 7.0 Hz, 1.0 Hz, phenyl imido para proton), 6.9 (mult, *o*-$(Me_3SiN)_2C_6H_4$ protons, 2 H), 7.05 (t, 8.0 Hz, phenyl imido meta protons, 2 H), 7.3 (ov, mult, *o*-$(Me_3SiN)_2$-C_6H_4 protons and phenyl imido ortho protons, 4 H). ^{13}C NMR (C_6D_6, 20 °C): δ 1.1, 2.7, 124.0, 124.2, 124.6, 125.0, 129.2, 135.0, 158.2, 203.4. Anal. Calcd for $C_{26}H_{45}MoN_3Si_4$: C, 51.37; H, 7.46; N, 6.91. Found: C, 51.13; H, 7.00; N, 7.03.

Computational Studies. Density functional theory (DFT) calculations were performed using the Gaussian 98W program package.[39] For model compound **4**, structures were optimized using Becke's hybrid three-parameter functional (B3LYP)[40] and the Los Alamos effective core potential (ECP) plus a standard double-ζ basis set (LANL2DZ)[41−43] to describe the molybdenum and the Dunning/Huzinaga full double-ζ basis set (D95)[44] to describe all other atoms. Calculations were performed with default pruned fine grids for gradients and Hessians and default SCF convergence for geometry optimizations (10^{-8}). The transition state **TS 4** was optimized with the same method and basis set using the Berny optimization program implemented in Gaussian and an initial guess for the transition state generated from manual manipulation of the geometry using the MOLDEN program.[45] An intrinsic reaction coordinate calculation on **TS 4** confirmed this transition state linked the two minima on the potential energy surface.

Energetics represented in this paper were validated by single-point energy calculations at the B3LYP level of theory and the LANL2DZ+P basis set (where +P stands for the addition of polarization functions to the D95 basis set as implemented in the Gaussian 98W program), on structures optimized at the B3LYP/LANL2DZ level. Relative energies represented in this work are electronic energies and do not include zero-point corrections. Vibrational frequency calculations were performed on the stationary points to confirm their existence as minima (number of imaginary frequencies = 0 or maxima (transition structures) # imaginary frequencies = 1, and to analyze (MOs)).

Model compound **5** was optimized by a two-layer ONIOM approach, in which the inner layer was model compound **4**, which is a simplified version of **3**, where the *o*-phenylene group (*o*-C_6H_4) that links the two N atoms of the diamido ligand was reduced to a −CH=CH− carbon chain. The organic groups on the nitrogen atoms ($SiMe_3$ of the amido and phenyl group of the imido) were replaced by hydrogen atoms for simplicity. Propyne was used as the alkyne fragment in this model. The outer layer consisted of the entire complex, including substituents on the imido and diamide ligands: i.e., the phenyl and $SiMe_3$ groups as well as the *o*-pda backbone.

Optimizations of model compound **5** and **TS 5** were performed with Becke's hybrid three-parameter functional (B3LYP),[40] for both layers. The inner layer was optimized with the LANL2DZ basis set on all atoms, while the outer layer was optimized with the LANL2MB basis set on all atoms in the outer layer, including all substituents an the imido and diamido ligands. Single-point energies were performed using the LANL2DZ basis set on the complete ONIOM optimized system. TS's were optimized using the Berny optimization program implemented in Gaussian, and an initial guess for the transition state was generated from manual manipulation of the geometry using the MOLDEN program. Orbital populations were analyzed with the NBO analysis of Weinhold et al.[36−38] as implemented in the Gaussian 98W software package. Structural diagrams and molecular orbital plots were obtained with the MOLDEN program.

Acknowledgment. We wish to acknowledge the National Science Foundation (Grant No. CHE-0094404) for the support of this work. K.A.A. wishes to acknowledge the National Science Foundation and the University of Florida for funding of the purchase of the X-ray equipment.

Supporting Information Available: Full details for experimental procedures and crystallographic data for compound **3e**, including tables of crystal data and data collection parameters, atomic coordinates, anisotropic displacement parameters, and all bond lengths and bond angles; XYZ files for **4, 5**, **TS 4**, and **TS 5** are also provided, along with a CIF file for **3e**. This material is available free of charge via the Internet at http://pubs.acs.org.

OM049942T

(39) Frisch, M. J.; Trucks, G. W.; Schlegel, H. B.; Scuseria, G. E.; Robb, M. A.; Cheeseman, J. R.; Zakrzewski, V. G.; Montgomery, J. A., Jr.; Stratmann, R. E.; Burant, J. C.; Dapprich, S.; Millam, J. M.; Daniels, A. D.; Kudin, K. N.; Strain, M. C.; Farkas, O.; Tomasi, J.; Barone, V.; Cossi, M.; Cammi, R.; Mennucci, B.; Pomelli, C.; Adamo, C.; Clifford, S.; Ochterski, J.; Petersson, G. A.; Ayala, P. Y.; Cui, Q.; Morokuma, K.; Rega, N.; Salvador, P.; Dannenberg, J. J.; Malick, D. K.; Rabuck, A. D.; Raghavachari, K.; Foresman, J. B.; Cioslowski, J.; Ortiz, J. V.; Baboul, A. G.; Stefanov, B. B.; Liu, G.; Liashenko, A.; Piskorz, P.; Komaromi, I.; Gomperts, R.; Martin, R. L.; Fox, D. J.; Keith, T.; Al-Laham, M. A.; Peng, C. Y.; Nanayakkara, A.; Challacombe, M.; Gill, P. M. W.; Johnson, B. G.; Chen, W.; Wong, M. W.; Andres, J. L.; Gonzalez, C.; Head-Gordon, M.; Replogle, E. S.; Pople, J. A. *Gaussian 98W*; Gaussian, Inc., Pittsburgh, PA, 2001.
(40) Becke, A. D. *J. Chem. Phys.* **1993**, *98*(2), 1372−1377.
(41) Hay, P. J.; Wadt, W. R. *J. Chem. Phys.* **1985**, *82*(1), 270−283.
(42) Wadt, W. R.; Hay, P. J. *J. Chem. Phys.* **1985**, *82*(1), 284−298.
(43) Hay, P. J.; Wadt, W. R. *J. Chem. Phys.* **1985**, *82*(1), 299−310.
(44) Dunning, T. H., Jr.; Hay, P. J. *Modern Theoretical Chemistry*; Plenum: New York, 1976; Vol. 3, p 1.
(45) Schaftenaar, G.; Noordik, J. H. *J. Computer-Aided Mol. Design* **2000**, *14*(2), 123−134.